

## Power Stability Analysis of Power Grid under PV Integration with STATCOM

**G.Naveen Kumar**

M.Tech-Energy Systems,  
Dept of Electrical Engineering,  
JBIET-Hyderabad,  
Telangana, India.

**S.Rathna Kumar**

Assistant Professor,  
Department of EEE,  
JBIET-Hyderabad,  
Telangana, India.

**R.Suresh Babu**

Associate Professor & HOD  
Department of EEE,  
JBIET-Hyderabad,  
Telangana, India.

### Abstract:

Grid connected renewable energy-based generation are deploying in recent years for many economic and environmental reasons. Static analysis is used to analyze the voltage stability of the system under study, while the dynamic analysis is used to evaluate the performance of compensators. In this paper one of the FACTS controller devices STATCOM is used to improve the voltage regulation thereby the power system stability. The PV-STATCOM improves the stable transmission limits substantially in the night and in the day even while generating large amounts of real power. The objective of this paper is only to demonstrate a new concept of using a PV solar farm inverter as a STATCOM using these reasonably good controller parameters. The above proposed model has been analyzed under various operating conditions and the performance of the model is evaluated using MATLAB/Simulink software.

### I. INTRODUCTION:

The principal benefit of the STATCOM for transient stability enhancement is direct through rapid bus voltage control. In particular, the STATCOM may be used to enhance power transfer during low-voltage conditions, which typically predominate during faults, decreasing the acceleration of local generators. An additional benefit is the reduction of the demagnetizing effects of faults on local generation.

STATCOMs behave analogously to synchronous compensators, except that STATCOMs have no mechanical inertia and are therefore capable of responding much more rapidly to changing system conditions. When compared to synchronous machines, they do not contribute to short circuit currents and have no moving parts. However, the system has a symmetric lead-lag capability and can theoretically go from full lag to full lead in fraction of cycles. In Many research papers, it has been shown that an energy storage system (ESS) plays an important role in power system control. In practice, by integrating an ESS with STATCOM (STATCOM + ESS) significant improvements over traditional STATCOM performance are achievable.

Some of the advantages of battery technologies are of higher energy storage densities, greater cycling capabilities, better reliability, and lower cost. This combined system is capable of mitigating majority of the stability and voltage fluctuation problems in the power system as discussed in detail in Section 2, with comprehensive literature review. A STATCOM, connected in shunt, with the system is capable of improving transient stability by compensating the reactive power at the point of common connection. The ultimate objective of applying reactive shunt compensation in a transmission system is to increase the transmittable power during transients.

This is achieved by increasing (decreasing) the power transfer capability when the machine angle increases (decreases). In Figure 1, which shows the single line diagram of a STATCOM, if the DC capacitor voltage,  $V_{DC}$ , is increased from its nominal value, the STATCOM is “overexcited” (capacitive mode) and generates reactive power. If the voltage of the DC capacitor bank is decreased below the nominal value, the STATCOM is “under excited” (inductive mode) and absorbs reactive power from the system. This is completely analogous to increasing or decreasing the field voltage of a synchronous compensator

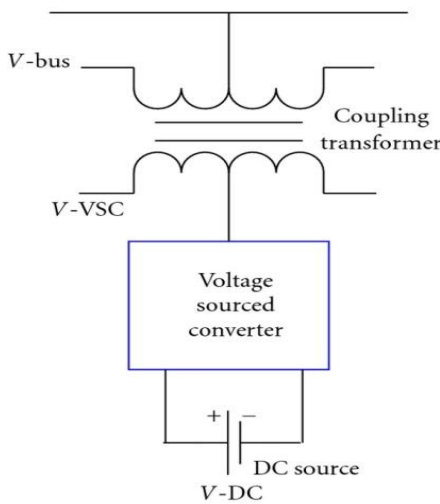


Fig 1: STATCOM

II. SYSTEM MODELLING:

The synchronous generator is represented by a detailed six thorder model and a DC1A-type exciter. The transmission-line segments  $TL_1$ ,  $TL_2$ ,  $TL_{11}$ ,  $TL_{12}$ , and  $TL_{22}$ , shown in Fig. 1, are represented by lumped pi-circuits. The PV solar DG is modeled as an equivalent voltage-source inverter along with a controlled current source as the dc source which follows the  $I-V$  characteristics of PV panels. The wind DG is likewise modeled as an equivalent voltage-source inverter. In the solar DG, dc power is provided by the solar panels, whereas in the full-converter-based wind DG, dc power comes out of a controlled ac-dc rectifier connected to the PMSG wind turbines, depicted as “wind Turbine-Generator-Rectifier(T-G-R).”

A maximum power point tracking (MPPT) algorithm based on an incremental conductance algorithm is used to operate the solar DGs at its maximum power point all of the time and is integrated with the inverter controller. The wind DG is also assumed to operate at its maximum power point, since this proposed control utilizes only the inverter capacity left after the maximum power point operation of the solar DG and wind DG.

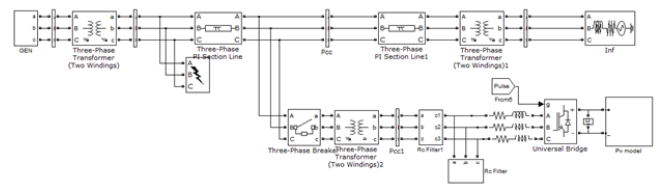


Fig 1: simulation diagram of study system with a single solar farm

For PV-STATCOM operation during nighttime, the solar panels are disconnected from the inverter and a small amount of real power is drawn from the grid to charge the dc capacitor. The voltage-source inverter in each DG is composed of six insulated-gate bipolar transistors (IGBTs) and associated snubber circuits as shown in Fig. 1. An appropriately large dc capacitor of size 200 Farad is selected to reduce the dc side ripple. Each phase has a pair of IGBT devices which converts the dc voltage into a series of variable-width pulsating voltages, using the sinusoidal pulse width modulation (SPWM) technique. An L-C-L filter is also connected at the inverter ac side.

III. CONTROL STRATEGY:

1) Conventional Reactive Power Control: The conventional reactive power control only regulates the reactive power output of the inverter such that it can perform unity power factor operation along with dc-link voltage control. The switching signals for the inverter switching are generated through two current control loops in d-q-0 coordinate system. The inverter operates in a conventional controller mode only provided that “Switch-2” is in the “OFF” position.

In this simulation, the voltage vector is aligned with the quadrature axis, that is,  $V_d=0$  hence,  $Q_{ref}$  is only proportional to  $I_d$  which sets the reference  $I_{d\_ref}$  for the upper control loop involving PI1. Meanwhile, the quadrature axis component  $I_q$  is used for dc-link voltage control through two PI controllers (PI-2 and PI-3) shown in Fig. 2 according to the set point voltage provided by the MPPT and injects all available real power “P” to the network. To generate the proper IGBT switching signals ( $g_{t1}$ ,  $g_{t2}$ ,  $g_{t3}$ ,  $g_{t4}$ ,  $g_{t5}$ ,  $g_{t6}$ ), the dq-components of the modulating signal are converted into three-phase sinusoidal modulating signals and compared with a high-frequency (5-kHz) fixed magnitude triangular wave or carrier signal.

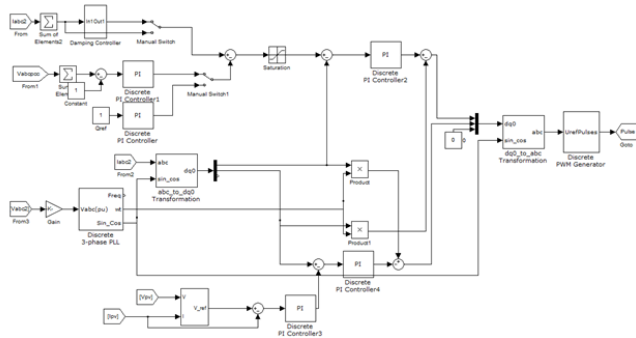


**Fig 2: Damping controller and PCC voltage-control system**

**PCC Voltage Control:** In the PCC voltage control mode of operation, the PCC voltage is controlled through reactive power change between the DG inverter and the grid. The conventional “Q” control channel is replaced by the PCC voltage controller in Fig. 2, simply by switching “Switch-1” to the position “A.” Hence, the measured signal  $V_{pccat}$  at the PCC is compared with the preset reference value  $V_{pcc\_ref}$  and is passed through the PI regulator, PI-4, to generate  $I_{d\_ref}$ . Damping Control-A novel auxiliary damping controller is added to the PV control system and shown in Fig. 2. This controller utilizes line current magnitude as the control signal. The output of this controller is added with the signal  $I_{d\_ref}$ .

**IV. SIMULATION RESULTS:**

The Simulation system is considered as two-area system, area-1 and area-2 as shown in Figure 3. The two areas are connected by two parallel connected long transmission lines. The direction of real power flow is from area-1 to area-2. The STATCOM is placed on one of the transmission lines and near to the generator being analyzed (area-1).

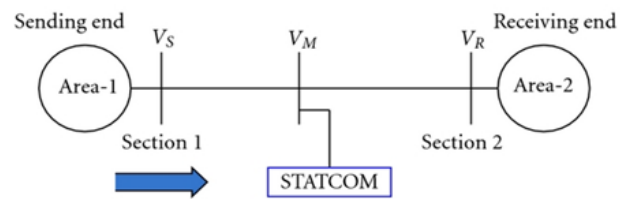
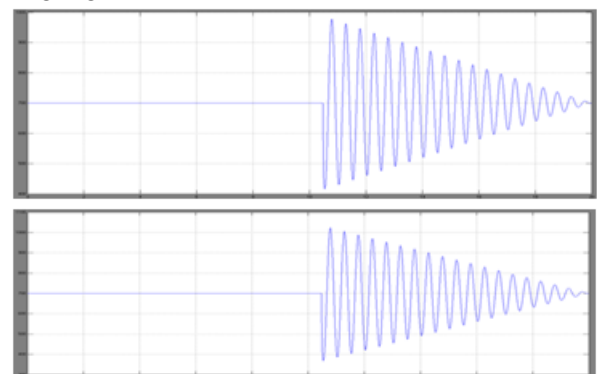


**Fig 3: Two-area system with STATCOM device Conventional reactive power control with novel damping control**

The solar DG is assumed to operate with its conventional reactive power controller and the DG operates at near unity power factor. For the nighttime operation of solar DG, the dc sources (solar arrays) are disconnected, and the solar DG inverter is connected to the grid using appropriate controllers, as will be described. Power transmission limits are now determined for the following four cases.

**Solar DG Operation during Night with Conventional Reactive Power Controllers**

The maximum stable power output from the generator is 731 MW when the solar DG is simply sitting idle during night and is disconnected from the network.



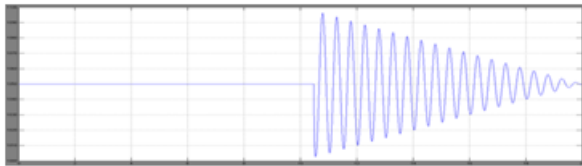


**Fig 4: Maximum nighttime power transfer and Voltage from the generator when solar DG remains idle**

**Solar DG Operation during the Night with Damping Controllers**

The quantities, and are illustrated in Fig. 5. The damping controller utilizes the full rating of the DG inverter at night to provide controlled reactive power and effectively damps the generator rotor-mode oscillations. The voltages at generator bus and at the PCCbus are depicted in Fig. 5. A very small amount of negative power flow from the solar farm is observed during nighttime.

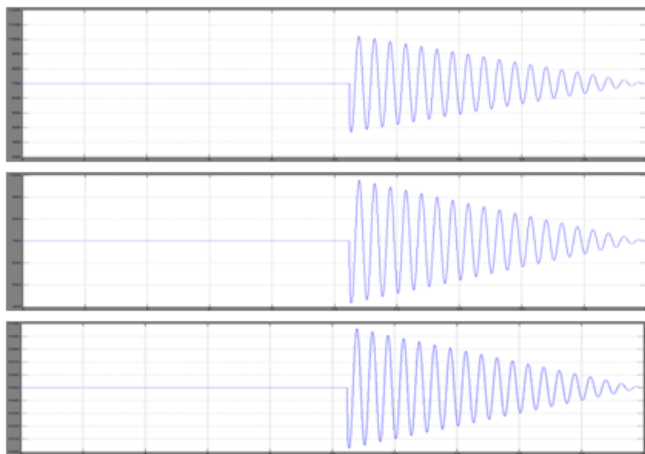


**Fig 5: Maximum nighttime power transfer and Voltages from the generator with solar DG using the damping controller**

**Solar DG Operation during the Day with a Damping Controller**

The quantities  $P_g$ ,  $P_{inf}$ ,  $P_{solar}$  are shown for the cases without the damping controller and with the damping controller in Figs. 6 and 7, respectively.

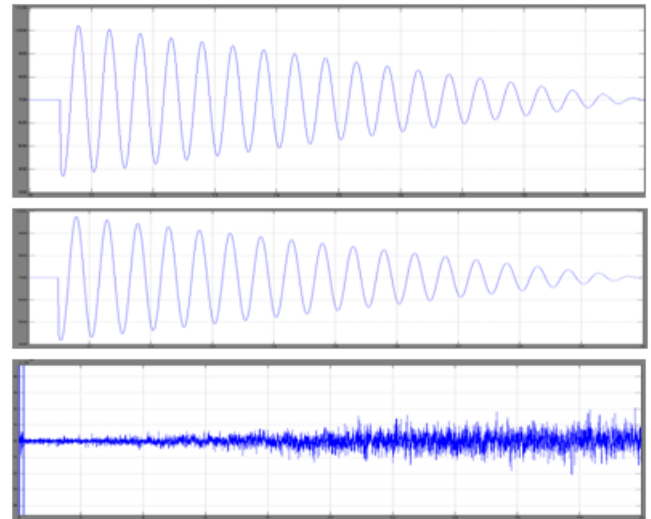


**Fig 6: Maximum daytime power transfer (719 MW) from the generator with solar DG generating 91-MW real power**

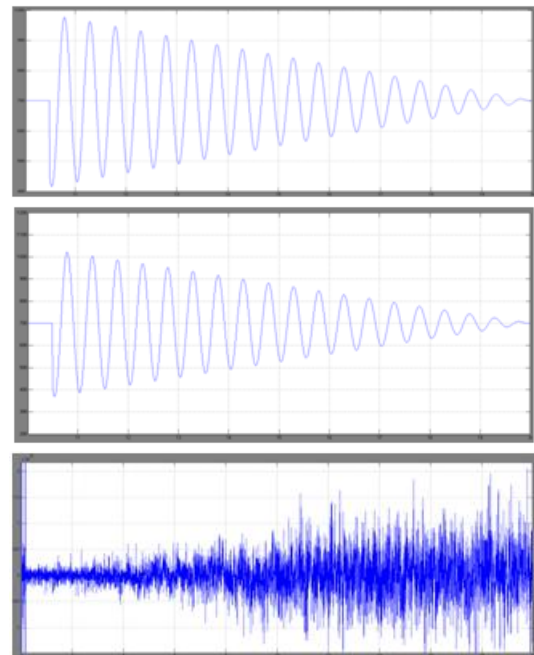


**Fig 7: Maximum daytime power transfer (861 MW) from the generator with solar DG generating 91-MW real power and using the damping controller**

**V. STABILITY ANALYSIS BY TWO-AREA WIND ENERGY CONVERSION SYSTEMS**

Economic Aspect of the BESS System Connected to STATCOM



The cost of such an integrated system can be broken down into three major segments, namely, the energy storage system, the supporting systems such as “refrigeration for SMES,” and the power conversion system. The amount of energy to be stored primarily determines the cost of the energy storage system. For the high-power low-energy storage applications, the configuration and the size of the power conversion system may become a dominant component.

In order to establish a realistic cost estimate, the following steps must be considered. (i) Identification of the system issue(s) to be addressed. (ii) Study of preliminary system characteristics. (iii) Define basic energy storage, power, voltage, and current requirements. (iv) Define utility financial benefits from the integration of the systems to determine adequacy of utility’s return on investment. (v) Model system performance in response to system demands to establish effectiveness of the BESS. (vi) Optimize integrated system specifications and determine system cost. (vii) Study and compare various energy storage systems performance and costs.

In terms of per unit active or reactive power, the cost of energy storage in feasible range is possible to be achieved by a FACTS + BESS system. While each system will be tailored to individual utility needs, target costs for a basic energy storage system on a per-kilowatt basis are less than the costs on a per-kilowatt basis of the lowest cost generation units. With advancement in utility scale battery storage system, cost has been going down and bigger battery size is practical.

**Simulation Analysis**  
**Wind Energy Integration**

Simulation analysis is performed in order to investigate the impact of STATCOM on the performance of a wind farm connected to the grid when a two-phase-to-line ground fault is applied to the system at time 20 seconds and the fault is cleared at time 20.3 seconds.

Figure 8 shows the results of bus voltage, active and reactive power at the bus where wind farm is connected.

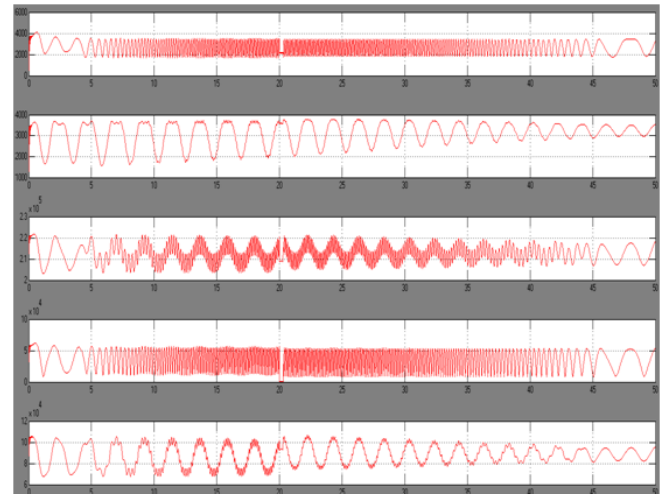


**Fig8: Wind Farm simulation without STATCOM connected to power transmission system**

**Stability Enhancement:**

The system response for fault-clearing times 0.3 sec, 0.35 sec is plotted and compared with faultless system. For the fault clearing time 0.3 sec, which is less than the critical clearing time 0.315 sec, the rotor angle of the generator will remain stable after the fault is cleared. For the fault clearing time 0.35 sec, which is greater than the critical clearing time 0.315 sec, the rotor angle of the generator becomes unstable after the fault is cleared. Since this case does not have any compensator attached to the AC system, STATCOM real and reactive powers are zero.

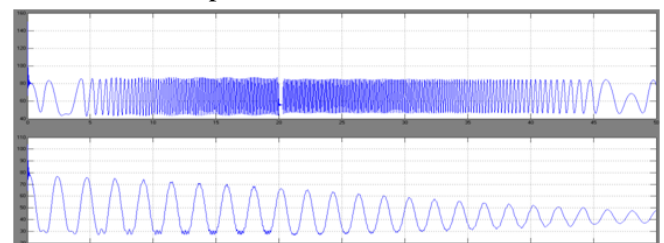


**Fig 9: Rotor angles response for different values of fault-clearing time**

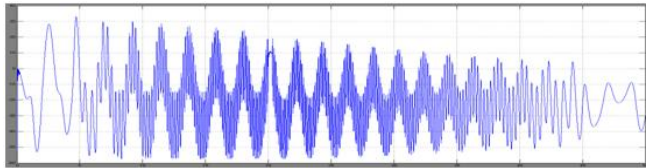


**Fig 10: Rotor angle difference without STATCOM**

## VI. CONCLUSION:

The importance and technical significance of BESS with STATCOM is elaborated here. Advantages of using BESS in connection to STATCOM in the power system for minimizing the transient dynamics of the power system with practical application is discussed in the latter half of the paper. This paper is majorly divided into two sections. In the first section, thorough reviews of the benefits of using STATCOM in conjunction with battery energy storage systems are discussed. It should also be noted that in this study the STATCOM provides a real power flow path for battery, but the operation of the battery is independent of the STATCOM controller. While the STATCOM is controlled to absorb or inject reactive power, the battery is controlled to absorb or inject real power. Detailed MATLAB/Simulink modeling and control of the integration of a STATCOM with a battery, and its dynamic response to generator rotor angle oscillations caused by a 3-phase fault as well as for integration of renewable energy are presented and discussed.

## REFERENCES:

- [1] R. M. Mathur and R. K. Varma, Thyristor-Based FACTS Controllers for Electrical Transmission Systems, Hoboken, NJ, USA: Wiley/IEEE, 2002.
- [2] S. A. Rahman, R. K. Varma, and W. Litzemberger, "Bibliography of FACTS applications for grid integration of wind and PV solar power systems: 1995–2010, IEEE working group report," presented at the IEEE Power Energy Soc. Gen. Meeting, Detroit, MI, USA, Jul. 2011.
- [3] Y. Xiao, Y. H. Song, C.-C. Liu, and Y. Z. Sun, "Available transfer capability enhancement using

FACTS devices," IEEE Trans. Power Syst., vol. 18, no. 1, pp. 305–312, Feb. 2003.

[4] Cross Texas Transmission, Salt fork to gray project. 2014. [Online]. Available: <http://www.crosstexas.com/SFWind.html>

[5] R. K. Varma, V. Khadkikar, and R. Seethapathy, "Nighttime application of PV solar farm as STATCOM to regulate grid voltage," IEEE Trans. Energy Convers., vol. 24, no. 4, pp. 983–985, Dec. 2009.

[6] R. K. Varma and V. Khadkikar, "Utilization of solar farm inverter as STATCOM," U.S. Provisional Patent, Sep. 15, 2009.

[7] R. K. Varma, S. A. Rahman, and R. Seethapathy, "Novel control of grid connected photovoltaic (PV) solar farm for improving transient stability and transmission limits both during night and day," in Proc. World Energy Conf., Montreal, QC, Canada, 2010, pp. 1–6.

[8] R. A. Walling and K. Clark, "Grid support functions implemented in utility-scale PV systems," in Proc. IEEE Power Energy Soc, Transm. Distrib. Conf. Expo., 2010, pp. 1–5.

[9] F. L. Albuquerque, A. J. Moraes, G. C. Guimaraes, S. M. R. Sanhueza, and A. R. Vaz, "Photovoltaic solar system connected to the electric power grid operating as active power generator and reactive power compensator," Solar Energy, vol. 84, no. 7, pp. 1310–1317, Jul. 2010.

[10] A. Beekmann, J. Marques, E. Quitmann, and S. Wachtel, "Wind energy converters with FACTS Capabilities for optimized integration of wind power into trans. and dist. systems," in Proc. CIGRE, Calgary, AB, Canada, 2009.